

# Toward Elimination of Discrepancies between Theory and Experiment: Anharmonic Rotational–Vibrational Spectrum of Water in Solid Noble Gas Matrices

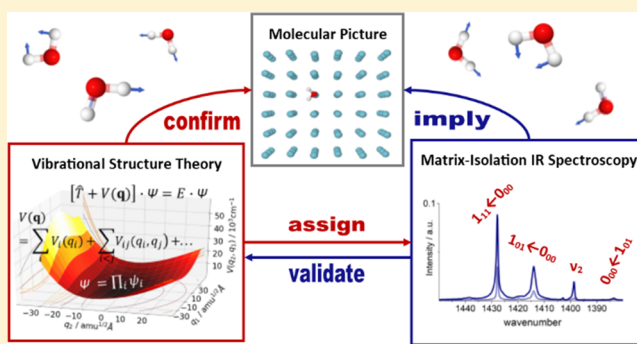
Dennis F. Dinu,<sup>†,‡,§</sup> Maren Podewitz,<sup>‡</sup> Hinrich Grothe,<sup>\*,§</sup> Klaus R. Liedl,<sup>\*,‡</sup> and Thomas Loerting<sup>\*,†</sup>

<sup>†</sup>Institute of Physical Chemistry and <sup>‡</sup>Institute of General, Inorganic and Theoretical Chemistry, University of Innsbruck, A-6020 Innsbruck, Austria

<sup>§</sup>Institute of Materials Chemistry, TU Wien, A-1060 Vienna, Austria

## Supporting Information

**ABSTRACT:** Rotational–vibrational spectroscopy of water in solid noble gas matrices has been studied for many decades. Despite that, discrepancies persist in the literature about the assignment of specific bands. We tackle the involved rotational–vibrational spectrum of the water isotopologues  $\text{H}_2^{16}\text{O}$ ,  $\text{HD}^{16}\text{O}$ , and  $\text{D}_2^{16}\text{O}$  with an unprecedented combination of experimental high-resolution matrix isolation infrared (MI-IR) spectroscopy and computational anharmonic vibrational spectroscopy by vibrational configuration interaction (VCI) on high-level ab initio potential energy surfaces. With VCI, the average deviation to gas-phase experiments is reduced from  $>100$  to  $\approx 1$   $\text{cm}^{-1}$  when compared to harmonic vibrational spectra. Discrepancies between MI-IR and VCI spectra are identified as matrix effects rather than missing anharmonicity in the theoretical approach. Matrix effects are small in Ne ( $\approx 1.5$   $\text{cm}^{-1}$ ) and a bit larger in Ar ( $\approx 10$   $\text{cm}^{-1}$ ). Controversial assignments in Ne MI-IR spectra are resolved, for example, concerning the  $\nu_3$  triad in HDO. We identify new transitions, for example, the  $\nu_2$   $1_{01} \leftarrow 1_{10}$  transition in  $\text{D}_2\text{O}$  and  $\text{H}_2\text{O}$  or the  $\nu_3$   $0_{00} \leftarrow 1_{01}$  transition in  $\text{D}_2\text{O}$ , and reassign bands, for example, the band at  $3718.9$   $\text{cm}^{-1}$  that is newly assigned as the  $1_{10} \leftarrow 1_{11}$  transition. The identification and solution of discrepancies for a well-studied benchmark system such as water prove the importance of an iterative and one-hand combination of theory and experiment in the field of high-resolution infrared spectroscopy of single molecules. As the computational costs involved in the VCI approach are reasonably low, such combined experimental/theoretical studies can be extended to molecules larger than triatomics.



## 1. INTRODUCTION

Water in the gas phase is of key importance in several fields, including engineering, meteorology, astrochemistry, and physical chemistry. Water molecules are abundant in Earth's atmosphere and play a crucial role in cloud formation, the hydrologic cycle, and climate. Water is an important greenhouse gas, closing large parts of the IR window of the atmosphere to space. It efficiently absorbs thermal radiation from Earth's surface but also from incoming sunlight. Without atmospheric water, Earth would be in a permanent ice age. Its identification in the atmosphere and in space is possible by its spectroscopic properties, based on rotational–vibrational spectroscopy and on microwave spectroscopy.<sup>1,2</sup> Pure rotational spectra<sup>3,4</sup> and IR spectra<sup>5,6</sup> are also used for remote detection. Water is a simple, triatomic, asymmetric rotator with  $C_{2v}$  symmetry, yet its spectra are highly complex. In the gas-phase, symmetric stretch ( $\nu_1$ ), asymmetric stretch ( $\nu_3$ ), and bending ( $\nu_2$ ) of the covalent bonds are coupled to rotations. Combination bands and overtones complicate the picture even

more. The spectroscopic complexity of water in the gas-phase is reflected in a comprehensive summary by the IUPAC.<sup>6–9</sup> In 1957, Pimentel et al. isolated water in an inert  $\text{N}_2$  matrix at 20 K,<sup>10</sup> providing the first matrix isolation infrared (MI-IR) spectrum. After this pioneering study, single molecule spectroscopy of water has seen a bloom<sup>11,12,21,13–20</sup> where MI has emerged as the standard for the study of the water monomer, the water dimer, and higher oligomers. In the atmosphere, the identification of the dimer has been a challenge as there is a strong overlap of monomer and dimer bands. It was only possible in 2003 through IR spectroscopy<sup>22</sup> (for a review, see Mukhopadhyay et al.<sup>23,24</sup>). In contrast to gas-phase IR, MI-IR spectroscopy allows for a dissection of the water monomer and its oligomers. However, the rotation of the water molecule in a cage of noble gas atoms and matrix

Received: July 29, 2019

Revised: August 8, 2019

Published: August 21, 2019

splitting of bands caused by different cage geometries have been a continuous source of debate and reassignments. Also, complexes of water, for example, the  $\text{H}_2\text{O}\cdot\text{N}_2$  cluster, have been considered to assign all observed bands.<sup>25,26</sup> Water is one of the most studied molecules in MI-IR, with experimental insights available for a wide range of different conditions, for example, different matrix materials, different temperatures, different isotopes, or in the presence of added dopants.<sup>11,12,25–34,13–15,17–21</sup> A recent historical overview is given by Ceponkus et al.<sup>32</sup> For the Ar matrix, the rotational–vibrational assignments for  $\text{H}_2^{16}\text{O}$ ,  $\text{HD}^{16}\text{O}$ , and  $\text{D}_2^{16}\text{O}$  are summed up by Engdahl and Nelander,<sup>33</sup> and a more recent study of  $\text{H}_2^{16}\text{O}$  is given by Perchard.<sup>27</sup> For the Ne matrix, a comprehensive assignment is reported by Forney et al.<sup>28</sup>

The rotational–vibrational spectrum is in theory derived by solving the nuclear Schrödinger equation. For a simple triatomic system such as water, sophisticated theoretical predictions are available,<sup>35–38</sup> with global potential energy surfaces (PES) calculated at a very high level of electronic structure theory and empirical refinement, while the exact solution of the nuclear Schrödinger equation provides a full line list of rotational–vibrational transitions that agree with gas-phase spectra within hundredths of a wavenumber. Such approaches yield the most accurate computational results possible and are strongly required, for example, in the field of astrochemistry. Considering water in noble gas matrices, tailor-made exact models were reported,<sup>32</sup> too. However, exact approaches are tedious to implement, and thus, they are not necessarily flexible, that is, not universally applicable but specific for the molecule under study. In order to be able to understand single molecule spectra in the matrix, a compromise needs to be found that provides sufficient accuracy on the theory side to allow for a sound assignment of experimentally observed bands. Ideally, the computation is efficient enough so that the method is suitable for a variety of molecules, also larger than triatomics. That is, computational approaches are needed that combine efficiency and accuracy yet also rigor and flexibility. When it comes to molecular identification by infrared spectroscopy, it is common to rely on computed vibrational spectra that are routinely predicted within the harmonic approximation (HA). Its inherent theoretical shortcomings are well known.<sup>39</sup> The most prominent drawback of the HA is its inaccuracy—vibrational frequencies are generally overestimated, with an error bar larger than the spectral range of the vibrational transitions. In order to compare HA spectra with experimental spectra, the easiest yet least rigorous practice is to shift the entire calculated HA spectrum with respect to the most intense band in the experimental spectrum by a specific scaling factor taken from the literature. As anharmonicity is specific for each vibration, such a linear scaling fails to correct for the whole calculated spectrum. The approach of scaled quantum mechanics<sup>40</sup> provides a theoretically more rigorous route to improve the accuracy, while flexibility is somewhat reduced, as the improvement is based on empirical refinement and, thus, biased toward an underlying experimental data set. In theoretical spectroscopy, two rigorous models that go beyond the HA received particular attention: the vibrational perturbation theory (VPT2), as used within MI studies of water by Tremblay et al.,<sup>30,31</sup> and the vibrational self-consistent field (VSCF)<sup>41–43</sup> in combination with vibrational configuration interaction (VCI) based on multimode representations of the PES. A correlation-corrected VSCF approach was

demonstrated, for example, by Jung and Gerber for water oligomers.<sup>44</sup> Both approaches come with improved accuracy and retain flexibility and efficiency. They are comprehensively reviewed.<sup>45,46</sup> In the present work, we employ the VSCF/VCI approach by Rauhut et al.,<sup>47–50</sup> which is concisely described in the next section.

To this end, we not only perform VCI calculations ourselves but also report new MI-IR experiments of  $\text{H}_2^{16}\text{O}$ ,  $\text{HD}^{16}\text{O}$ , and  $\text{D}_2^{16}\text{O}$ . As matrix materials, we use argon, which is commonly used in the literature,<sup>11,12,25,27,13–15,17–21</sup> and neon, which is less frequently used,<sup>28–31</sup> as its low freezing point is technically challenging to handle. Our cutting-edge experimental MI-IR setup, with a vacuumed spectrometer, a high-quality light source and interferometer, and a liquid nitrogen cooled detector, allows for a very good signal/noise ratio that helps to detect even the weakest bands (see next section for more details). It should be stressed that water is a well-studied molecule. As mentioned above, state-of-the-art calculations provide extensive and highly accurate rotational–vibrational line lists. Those can be employed to investigate the MI-IR spectrum of water. However, with the one-hand combination of experiment and calculation in this work, we are in a position to perform an iterative assignment. We do not need to rely merely on literature data. The merit of such a combined approach becomes clear under the consideration that it can be extended to molecules where computationally predicted spectroscopic properties are not as accurately accessible as for the water molecule.

## 2. METHODOLOGY

**2.1. Experimental Spectrum by Matrix Isolation Infrared Spectroscopy.** The matrix isolation (MI) technique used in this study has been previously described by Grothe et al.<sup>51</sup> A detailed depiction of the apparatus is found in the Supporting Information of ref 52. The highlights of the setup are a  $180^\circ$  rotatable high-vacuum cryostat that can be cooled to 5.8 K, allowing for stable solid Ne matrices, and the FTIR spectrometer Vertex 80v (Bruker, Karlsruhe), which is operating under 2 mbar with a liquid-nitrogen-cooled MCT detector to eliminate all atmospheric noise in the infrared region. This is especially necessary when studying the infrared spectrum of the omnipresent water. The spectrometer itself is vibration-cushioned and uncoupled from the matrix isolation apparatus to avoid vibration-induction. The arising gap is constantly flushed with pure  $\text{N}_2$  gas. In all experiments, the atmospheric water is not observed with this setup. To record the spectra of water vapor trapped in the noble gas matrix, 512 scans are accumulated at a resolution of  $0.3\text{ cm}^{-1}$ .

We use a liquid sample of  $\text{D}_2\text{O}$  (99.96%, delivered by Eurisotop, D215ES, lot = Q2141, batch = BR575) in all experiments.  $\text{H}_2\text{O}$  and  $\text{HDO}$  species are generated spontaneously by isotope exchange with protons on the surface of the mixing chamber steel tubes. About 2.5 mL of the sample is added by a sterile syringe into a glass flask under argon flux to reduce contamination with atmospherically gases such as  $\text{H}_2\text{O}$ ,  $\text{CO}_2$ ,  $\text{O}_2$ , and  $\text{N}_2$ . The sample is mounted to the mixing chamber of the MI apparatus and herein degassed by multiple freeze and thaw procedures. Before mixing of the sample with a rare gas, the vapor above the liquid is evacuated in order to provide “freshly” evaporated chemicals. The gas mixture is then prepared by barometric monitoring within a volume of about 2 L that was previously evacuated at  $10^{-5}$  mbar. A mixture of 2 mbar sample gas in dilution with about 990–1010 mbar rare

gas is denoted as 1:500. We measure the spectra of 1:250, 1:500, and 1:1000 dilutions both in Ar and in Ne. The matrix is deposited onto a gold plate in the high-vacuum chamber at  $10^{-7}$  mbar and 5.8 K, generated by a Gifford-McMahon cooler.<sup>53</sup> The gas mixture is introduced at a constant flow of 4 mbar/min from a volume of about 200 mL and a pressure of 900–980 mbar, depending on the previously prepared mixture. The deposition time is about 45 min per matrix layer. As water adsorbs on the surface of the mixing chamber steel tubes, the initial ratio of dilution is somewhat altered. Hence, it is necessary to deposit up to three layers to produce a matrix containing enough water species for an intensive infrared spectrum. All IR spectra are recorded in the mid-infrared region of 4000–500  $\text{cm}^{-1}$ . Background spectra of the gold plate at 5.8 K are taken before each sample measurement. The spectra shown in Figure 2 are corrected for this background.

**2.2. Calculated Spectrum by Vibrational Self-Consistent Field and Configuration Interaction.** All calculations are performed with the MOLPRO software package.<sup>54,55</sup> In all that follows, the electronic structure is calculated with the coupled cluster ansatz including single, double, and perturbative triple excitations and the explicit correlation of interelectronic distances, that is, the CCSD(T)-F12 ansatz.<sup>56,57</sup>

This ansatz allows for a faster basis-set convergence than conventional coupled cluster approaches with little additional computational cost. The accuracy of this method with the here used triple- $\zeta$  (VTZ-F12) basis set<sup>58,59</sup> corresponds roughly to a conventional calculation with a quintuple- $\zeta$  basis set, which is sufficiently close to the complete basis-set limit. The Born–Oppenheimer equilibrium geometry of the water monomer, numerical second derivatives of the energy near the equilibrium, and the harmonic frequencies are obtained by using the MOLPRO default procedures `optg` and `freq`. This yields also the commonly known normal modes of the water molecule: asymmetric stretch  $q_3$ , symmetric stretch  $q_1$ , and in-plane bend  $q_2$ . These normal-modes  $q_i$  are used as a coordinate system for the subsequent calculation of a multimode representation of the potential energy surface (PES), a sum of one-mode (1D) potentials  $V(q_i)$ , two-mode (2D) potentials  $V(q_i, q_j)$ , and so forth, as depicted in Figure 1. The strongly anharmonic nature, especially of  $V(q_1)$ , is evident. The MOLPRO `surf` algorithm constructs the PES on a grid where each grid point is generated by elongation along the normal modes (1D), along two combined normal modes (2D), and so on. Symmetry considerations, iterative interpolation, and prescreening techniques significantly lower the amount of ab initio single point energy calculations, with negligible loss of accuracy in the final PES, as pioneered by Rauhut.<sup>47</sup> After testing various schemes for the PES construction, we find in accordance with the literature<sup>60</sup> that the use of the CCSD(T)-F12 level of theory in 1D, 2D, and 3D sub-potentials is preferable in terms of accuracy in the subsequently calculated vibrational spectrum. As the water molecule has a rather simple electronic structure, the CCSD(T)-F12 single point energy calculations are also not too expensive. Based on the multimode representation of the PES, the nuclear Schrödinger equation using the Watson operator is solved variationally within the VSCF<sup>41–43</sup> where the wave function is approximated as a Hartree product of one-mode functions. This approximated solution is subsequently correlation-corrected by the configuration-selective VCI.<sup>48,50</sup> This yields the VCI wave function as a linear combination of various excited Hartree products, with the anharmonic vibrational energies corre-

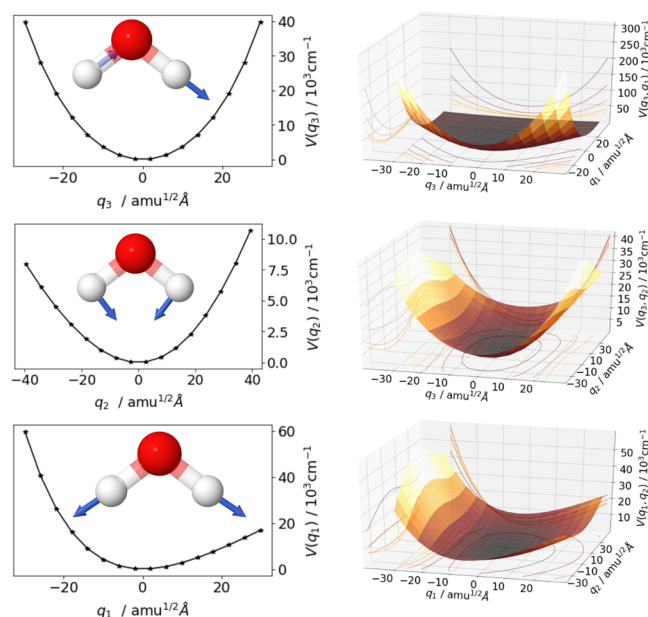


**Figure 1.** Potential energy surface of H<sub>2</sub>O. Grid representation of the multimode PES, calculated with CCSD(T)-F12/VTZ-F12. (left) One-mode sub-potentials  $V(q_i)$  with vector depiction of the normal-modes  $q_i$  of water. (right) Two-mode sub-potentials  $V(q_i, q_j)$ . Three-mode sub-potentials are not depicted yet considered in the calculation.

sponding to specific VCI states that inherit the nomenclature of the normal-mode picture. The nuclear wave function allows for the calculation of IR intensities by employing a multimode representation of the dipole moment surface. The latter is calculated at the HF/VTZ-F12 level of theory. The rotational fine structure is calculated within the adiabatic rotation approximation (ARA).<sup>61</sup> All these calculations are achieved by the `vscf` and `vci` algorithms that are provided in MOLPRO. In a fairly rough approximation, the R-Branch is considered as the mirror image of the P-Branch in close vicinity of the Q-Branch. In order to assign rotational–vibrational transitions from the initial state  $J''$  to the excited state  $J'$ , we use the spectroscopic nomenclature  $J'_{KaKc} \leftarrow J''_{KaKc}$  with  $J$  being the rotational quantum number and  $K_a$  and  $K_c$  being the projection quantum numbers of the asymmetric top.

### 3. RESULTS AND DISCUSSION

The results of our assignment in the MI-IR spectra are depicted in Figure 2a considering the Ne matrix and in Figure 2b considering the Ar matrix. The assignment is summed up in Tables 1 and 2. With a pure D<sub>2</sub><sup>16</sup>O sample, we simultaneously observe H<sub>2</sub><sup>16</sup>O, HD<sup>16</sup>O, and D<sub>2</sub><sup>16</sup>O in the spectrum due to proton exchange in the mixing chamber. In Ar, the H<sub>2</sub>O shows the weakest bands. D<sub>2</sub>O and HDO show higher intensities, inversely proportional to the sample dilution. The same holds for Ne, yet here, the intensities are lower overall. In both Ar and Ne MI-IR, we observe roughly 10 bands that can be accounted to water dimers (see Table S1 in the Supporting Information). All spectra exhibit multiple rotational–vibrational transitions (rovibs) with high intensities in the P-branch and a few less intense rovibs in the R-branch. In Ar, most of the pure vibrational transitions (vibs) are observed, whereas in Ne only two are observed, presumably because of the low overall intensity. Table 1 presents a comparison of the vibs between the HA and VCI calculations and experimental data

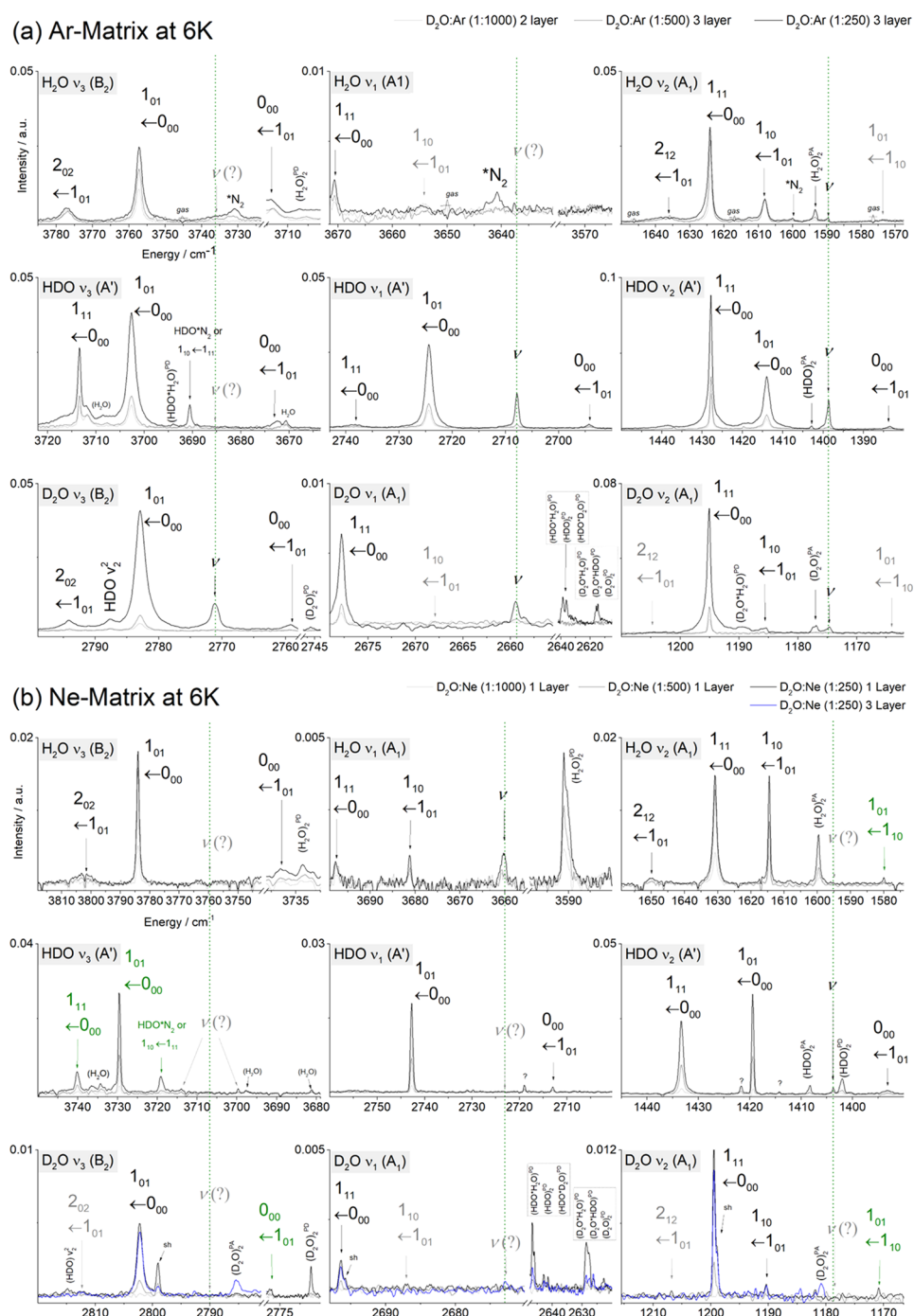


**Figure 2.** MI-IR spectrum of a D<sub>2</sub>O sample containing H<sub>2</sub>O and HDO, diluted 1:250, 1:500, and 1:1000 in (a) Ar and (b) Ne, both at 6 K. Pure vibrational transitions are labeled as  $\nu$  along the vertical dotted lines. Rotational–vibrational transitions are labeled as  $J'_{KaKc} \leftarrow J''_{KaKc}$  with  $J$  being the rotational quantum number and  $K_a$  and  $K_c$  being the projection quantum numbers of the asymmetric top. \*N<sub>2</sub> are supposedly due to a H<sub>2</sub>O\*N<sub>2</sub> complex. Water dimers are labeled as proton donor (PD) or proton acceptor (PA) vibrations. New or tentative assignments are marked in green. Expected bands from literature data are marked in gray.

(comprising the measured Ar and Ne MI-IR data here, some literature MI-IR data,<sup>17,28,32,33</sup> and literature gas-phase data.<sup>62–66</sup>) Table 2 presents a similar comparison, considering the rovibs. When compared to the gas-phase, it is immediately evident that the HA is far from being sufficient to reproduce the experiment. Considering the vibs, the mean absolute deviation (MAD) between HA and experiment amounts to 107.9 cm<sup>-1</sup>, with a maximum deviation (MAX) of 187.9 cm<sup>-1</sup>. In contrast, the VCI results perfectly agree with the gas-phase,

with an MAD of 1.1 cm<sup>-1</sup> (MAX = 1.6 cm<sup>-1</sup>). That is, the VCI approach results in a roughly 100-fold reduction of the discrepancy between experiment and theory. This has also been found for other molecules in the literature.<sup>60</sup> Also, when considering the 42 rovibs as listed in Table 2, the VCI results perfectly agree with the gas-phase, with an MAD of 1.1 cm<sup>-1</sup> (MAX = 5.7 cm<sup>-1</sup>). In view of the assignment of MI-IR spectra, we compare the VCI results with MI-IR data. For the vibs listed in Table 1, we observe with respect to the VCI

Table 1. Fundamental Vibrational Transitions of Water Monomers as Observed in Ar and Ne MI-IR at 6 K and Compared to Gas-phase Reference and the here Calculated Transitions<sup>a</sup>

Molecule	Assign.	Ar	Ne	Gas	VCI <sup>b</sup>	HA <sup>c</sup>
<b>H<sub>2</sub>O</b>	<i>v</i> <sub>3</sub> (B <sub>2</sub> )	3735.9 <sup>g</sup>	3759.5 <sup>f</sup>	3755.9 <sup>h</sup>	<b>3754.3</b>	<b>3943.8</b>
	<i>v</i> <sub>1</sub> (A <sub>1</sub> )	3638.0 <sup>g</sup>	<b>3660.5</b>	3657.1 <sup>h</sup>	<b>3656.5</b>	<b>3833.8</b>
	<i>v</i> <sub>2</sub> (A <sub>1</sub> )	<b>1589.9</b>	1595.6 <sup>e</sup>	1594.8 <sup>i</sup>	<b>1596.3</b>	<b>1650.6</b>
<b>HDO</b>	<i>v</i> <sub>3</sub> (A')	3685.7 <sup>d</sup>	3713.9 <sup>f</sup> 3699.6 <sup>e</sup>	3707.5 <sup>j</sup>	<b>3706.1</b>	<b>3890.9</b>
	<i>v</i> <sub>1</sub> (A')	<b>2707.9</b>	2722.9 <sup>e</sup>	2723.7 <sup>k</sup>	<b>2722.6</b>	<b>2824.5</b>
	<i>v</i> <sub>2</sub> (A')	<b>1398.6</b>	<b>1403.7</b>	1403.5 <sup>k</sup>	<b>1404.6</b>	<b>1446.8</b>
<b>D<sub>2</sub>O</b>	<i>v</i> <sub>3</sub> (B <sub>2</sub> )	<b>2771.2</b>	2790.0 <sup>f</sup>	2787.7 <sup>l</sup>	<b>2786.2</b>	<b>2889.3</b>
	<i>v</i> <sub>1</sub> (A <sub>1</sub> )	<b>2659.5</b>	2672.7 <sup>e</sup>	2671.7 <sup>l</sup>	<b>2671.2</b>	<b>2763.4</b>
	<i>v</i> <sub>2</sub> (A <sub>1</sub> )	<b>1174.7</b>	1178.7 <sup>e</sup>	1178.4 <sup>l</sup>	<b>1179.3</b>	<b>1208.1</b>
MAD		12.9	2.1	1.1	0	108.2
MAX		20.4	5.2	1.6	0	189.5

<sup>a</sup>Values in cm<sup>-1</sup>. Bold face: obtained in the present study. Italics: Reference data. <sup>b</sup>VCI(SDTQ) on a 3-mode PES at CCSD(T)-F12/VTZ-F12. <sup>c</sup>Harmonic Approximation at CCSD(T)-F12/VTZ-F12. <sup>d</sup>Ref 17. <sup>e</sup>Ref 28. <sup>f</sup>Ref 32. <sup>g</sup>Ref 33. <sup>h</sup>Ref 62. <sup>i</sup>Ref 63. <sup>j</sup>Ref 64. <sup>k</sup>Ref 65. <sup>l</sup>Ref 66.

results in Ar matrices an MAD of 12.9 cm<sup>-1</sup> (MAX of 20.4 cm<sup>-1</sup>) and in Ne matrices an MAD of 2.1 cm<sup>-1</sup> (MAX = 5.2 cm<sup>-1</sup>). The gas-phase and Ne matrix show similar MADs, whereas the MAD of the Ar matrix increases by a factor of 6. Similar conclusions can be drawn for the rovibs listed in Table 2. With respect to the VCI results, in Ar matrices, an MAD of 13.1 cm<sup>-1</sup> (MAX = 24.4 cm<sup>-1</sup>) and in Ne matrices an MAD of 3.2 cm<sup>-1</sup> (MAX = 7.9 cm<sup>-1</sup>) are found. In this case, an improvement of a factor of 4 is reached when using Ne instead of Ar. We can confirm that Ne matrices have little effect on the trapped water molecules, therefore being an excellent approximation to the gas-phase situation, whereas Ar does exert a vivid effect and is only a good approximation to the gas-phase situation. The mean matrix-shift incurred by changing from gas-phase (i.e., MAD wrt gas-phase) to Ar matrix of 13.2 cm<sup>-1</sup> (rovibs: 13.6 cm<sup>-1</sup>) and to Ne matrix of 1.5 cm<sup>-1</sup> (rovibs: 3.2 cm<sup>-1</sup>) is much smaller than the improvement gained by anharmonic VCI calculations compared to the HA, which is in mean roughly at 100 cm<sup>-1</sup>. This means that matrix-shifts, especially in the case of Ne matrices, are not problematic when the assignment is supported by VCI calculations. In other words, the correction for anharmonicity by the VCI approach, with an MAD of 1.1 cm<sup>-1</sup> with respect to the gas-phase, perfectly allows identification of matrix-shifts. In all cases, the largest discrepancies between theory and experiments (i.e., the MAX values) arise from the calculated rovibs within the adiabatic rotation approximation (ARA). The H<sub>2</sub>O molecule as an asymmetric top is known to be an unfavorable case for this method.<sup>61</sup> This holds especially with increasing quantum number *J*. However, as the here observed rovibs are *J* = 1 and *J* = 2, the results are still adequate. In general, this discrepancy is a minor issue for the investigation in MI-IR spectra, as this technique usually suppresses rotation completely. In fact, the water molecule is an exceptional case.

With the use of the VCI approach, we can confirm most of the transitions assigned in the literature and additionally identify bands that were previously not assigned. In Ne MI-IR, a band at 1580.0 cm<sup>-1</sup> can be assigned as H<sub>2</sub>O *v*<sub>2</sub> 1<sub>01</sub> ← 1<sub>10</sub> (VCI: 1578.9 cm<sup>-1</sup>) and another band at 1170.2 cm<sup>-1</sup> can be

assigned as D<sub>2</sub>O *v*<sub>2</sub> 1<sub>01</sub> ← 1<sub>10</sub> (VCI: 1169.1 cm<sup>-1</sup>). As the underlying normal-mode for both species have the same A<sub>1</sub> irrep, this assignment is also plausible from symmetry considerations. In previous Ne experiments,<sup>28</sup> the H<sub>2</sub>O *v*<sub>3</sub> 0<sub>00</sub> ← 1<sub>01</sub> transition is observed, yet the corresponding transition in D<sub>2</sub>O is not. We find a weak signal at 2778.7 cm<sup>-1</sup> that can be assigned as the D<sub>2</sub>O *v*<sub>3</sub> 0<sub>00</sub> ← 1<sub>01</sub> (VCI: 2773.9 cm<sup>-1</sup>). Furthermore, an inconsistency in the literature considering the HDO *v*<sub>3</sub>, *v*<sub>1</sub>, and *v*<sub>2</sub> can be resolved. The HDO normal-modes have the same A' irrep, and hence, we expect a similar band shape and assignment for all three spectral regions. In the HDO *v*<sub>1</sub> and *v*<sub>2</sub> region, the assignments in Ar MI-IR by Engdahl and Nelander<sup>33</sup> and in Ne MI-IR by Forney et al.<sup>28</sup> are consistent and also plausible from the symmetry considerations. In the HDO *v*<sub>3</sub> region, we observe a triad with an intensity of 1:5:1 in both Ar and Ne matrices. The assignment of these transitions by Engdahl and Nelander in Ar as 1<sub>11</sub> ← 0<sub>00</sub>, 1<sub>01</sub> ← 0<sub>00</sub>, and HDO\*N<sub>2</sub> differs from the assignment by Forney et al. in Ne as 2<sub>12</sub> ← 1<sub>01</sub>, 1<sub>11</sub> ← 0<sub>00</sub>, and 1<sub>10</sub> ← 1<sub>01</sub>. Our VCI calculations confirm the assignment given by Engdahl and Nelander, which is consistent within all three regions also from symmetry consideration. We adopt the assignment of the HDO *v*<sub>3</sub> region by Engdahl and Nelander also for the Ne MI-IR. One intriguing point still remains: The band at 3690.6 cm<sup>-1</sup> in Ar is given by Engdahl and Nelander<sup>33</sup> either as the HDO\*N<sub>2</sub> band or as the 1<sub>10</sub> ← 1<sub>11</sub> transition. In the Ne matrix, this band occurs at 3718.9 cm<sup>-1</sup> where it is assigned as 1<sub>11</sub> ← 0<sub>00</sub> by Forney et al. Based on our calculations, the 1<sub>10</sub> ← 1<sub>11</sub> transition is at the origin of this band and it is not necessary to invoke a N<sub>2</sub>-induced band. Other discrepancies in the assignment of the HDO species are noticeable between Forney et al.<sup>28</sup> and a more recent publication by Ceponkus et al.<sup>32</sup> The HDO *v*<sub>3</sub> is assigned at 3699.0 cm<sup>-1</sup> in ref 28 and at 3713.8 cm<sup>-1</sup> in ref 32. We observe both bands with almost identical but very weak intensities. Considering the VCI calculation, the band should in fact be located at neither of these two positions but in the middle between them (VCI: 3706.1 cm<sup>-1</sup>). Based on the good agreement between VCI calculation and the residual Ne MI-IR

**Table 2. Rotational-Vibrational Transitions of Water Monomers as Observed in Ar and Ne MI-IR at 6 K and Compared to Gas-phase Reference and the here Calculated Transitions<sup>a</sup>**

Molecule Vib. (Irrep.)	Branch	Rotation $J'_{KaKc} \leftarrow J''_{Ka}$ Kc	Ar	Ne	Gas	VCI <sup>b</sup>
<b>H<sub>2</sub>O</b> $\nu_3$ (B <sub>2</sub> )	P	2 <sub>02</sub> ←1 <sub>01</sub>	<b>3776.9</b>	<b>3801.5</b>	3801.7 <sup>h</sup>	<b>3801.3</b>
		1 <sub>10</sub> ←0 <sub>00</sub>			3797.0 <sup>h</sup>	<b>3796.2</b>
	R	1 <sub>11</sub> ←0 <sub>00</sub>			3791.7 <sup>h</sup>	<b>3791.1</b>
		1 <sub>01</sub> ←0 <sub>00</sub>	<b>3757.2</b>	<b>3784.0</b>	3779.5 <sup>h</sup>	<b>3778.4</b>
<b>H<sub>2</sub>O</b> $\nu_1$ (A <sub>1</sub> )	P	0 <sub>00</sub> ←1 <sub>01</sub>	<b>3711.8</b>	<b>3736.5</b>	3732.4 <sup>h</sup>	<b>3730.2</b>
		1 <sub>10</sub> ←0 <sub>00</sub>			3698.5 <sup>h</sup>	<b>3698.3</b>
	R	1 <sub>11</sub> ←0 <sub>00</sub>	<b>3670.6</b>	<b>3697.4</b>	3693.3 <sup>h</sup>	<b>3693.2</b>
		1 <sub>10</sub> ←1 <sub>01</sub>	3653.5 <sup>g</sup>	<b>3681.2</b>	3675.1 <sup>h</sup>	<b>3674.2</b>
<b>H<sub>2</sub>O</b> $\nu_2$ (A <sub>1</sub> )	P	1 <sub>01</sub> ←0 <sub>00</sub>			3680.4 <sup>h</sup>	<b>3680.6</b>
		2 <sub>12</sub> ←1 <sub>01</sub>	<b>1636.9</b>	<b>1650.2</b>	1653.3 <sup>i</sup>	<b>1652.1</b>
	R	1 <sub>10</sub> ←0 <sub>00</sub>			1640.5 <sup>i</sup>	<b>1638.2</b>
		1 <sub>11</sub> ←0 <sub>00</sub>	<b>1624.0</b>	<b>1630.9</b>	1635.0 <sup>i</sup>	<b>1633.1</b>
<b>HDO</b> $\nu_3$ (A')	P	1 <sub>01</sub> ←0 <sub>00</sub>			1618.6 <sup>i</sup>	<b>1620.4</b>
		1 <sub>10</sub> ←1 <sub>01</sub>	<b>1608.1</b>	<b>1614.5</b>	1616.7 <sup>i</sup>	<b>1614.1</b>
	R	0 <sub>00</sub> ←1 <sub>01</sub>	1573.1 <sup>g</sup>	<b>1580.0</b>	1572.8 <sup>i</sup>	<b>1578.5</b>
		1 <sub>10</sub> ←0 <sub>00</sub>			3738.9 <sup>j</sup>	<b>3738.2</b>
<b>HDO</b> $\nu_1$ (A')	P	1 <sub>11</sub> ←0 <sub>00</sub>	<b>3713.5</b>	<b>3740.1</b>	3736.2 <sup>j</sup>	<b>3735.6</b>
		1 <sub>01</sub> ←0 <sub>00</sub>	<b>3702.7</b>	<b>3729.6</b>	3722.9 <sup>j</sup>	<b>3721.7</b>
	R	0 <sub>00</sub> ←1 <sub>01</sub>	<b>3673.0</b>	-	3692.0 <sup>j</sup>	<b>3690.4</b>
		1 <sub>10</sub> ←0 <sub>00</sub>			2756.0 <sup>k</sup>	<b>2754.8</b>
<b>HDO</b> $\nu_2$ (A')	P	1 <sub>11</sub> ←0 <sub>00</sub>	<b>2738.1</b>	-	2753.3 <sup>k</sup>	<b>2752.2</b>
		1 <sub>01</sub> ←0 <sub>00</sub>	<b>2724.4</b>	<b>2742.8</b>	2738.9 <sup>k</sup>	<b>2738.3</b>
	R	0 <sub>00</sub> ←1 <sub>01</sub>	<b>2694.4</b>	<b>2713.0</b>	2708.4 <sup>k</sup>	<b>2707.0</b>
		1 <sub>10</sub> ←0 <sub>00</sub>			1438.2 <sup>k</sup>	<b>1436.8</b>
<b>HDO</b> $\nu_2$ (A')	P	1 <sub>11</sub> ←0 <sub>00</sub>	<b>1427.7</b>	<b>1433.3</b>	1435.3 <sup>k</sup>	<b>1434.2</b>
		1 <sub>01</sub> ←0 <sub>00</sub>	<b>1414.0</b>	<b>1419.4</b>	1419.0 <sup>k</sup>	<b>1420.3</b>
	R	0 <sub>00</sub> ←1 <sub>01</sub>	<b>1383.4</b>	<b>1389.3</b>	1387.9 <sup>k</sup>	<b>1389.0</b>
		2 <sub>02</sub> ←1 <sub>01</sub>	<b>2793.9</b>	2811.3 <sup>e</sup>	2811.3 <sup>i</sup>	<b>2810.1</b>
<b>D<sub>2</sub>O</b> $\nu_3$ (B <sub>2</sub> )	P	1 <sub>10</sub> ←0 <sub>00</sub>			2809.8 <sup>i</sup>	<b>2808.6</b>
		1 <sub>11</sub> ←0 <sub>00</sub>			2807.4 <sup>i</sup>	<b>2806.3</b>
	R	1 <sub>01</sub> ←0 <sub>00</sub>	<b>2783.0</b>	<b>2802.3</b>	2799.8 <sup>i</sup>	<b>2798.4</b>
		0 <sub>00</sub> ←1 <sub>01</sub>	<b>2759.3</b>	<b>2778.7</b>	2775.7 <sup>i</sup>	<b>2773.9</b>
<b>D<sub>2</sub>O</b> $\nu_1$ (A <sub>1</sub> )	P	1 <sub>10</sub> ←0 <sub>00</sub>			2694.0 <sup>i</sup>	<b>2693.7</b>
		1 <sub>11</sub> ←0 <sub>00</sub>	<b>2677.8</b>	<b>2696.3</b>	2691.6 <sup>i</sup>	<b>2691.3</b>
	R	1 <sub>10</sub> ←1 <sub>01</sub>	2667.3 <sup>g</sup>	2686.6 <sup>e</sup>	2682.1 <sup>i</sup>	<b>2681.4</b>
		1 <sub>01</sub> ←0 <sub>00</sub>			2683.6 <sup>i</sup>	<b>2683.4</b>
<b>D<sub>2</sub>O</b> $\nu_2$ (A <sub>1</sub> )	P	2 <sub>12</sub> ←1 <sub>01</sub>	1204.0 <sup>g</sup>	1206.7 <sup>e</sup>	1209.4 <sup>i</sup>	<b>1209.3</b>
		1 <sub>10</sub> ←0 <sub>00</sub>			1202.3 <sup>i</sup>	<b>1201.8</b>
	R	1 <sub>11</sub> ←0 <sub>00</sub>	<b>1195.1</b>	<b>1199.4</b>	1199.8 <sup>i</sup>	<b>1199.4</b>
		1 <sub>01</sub> ←0 <sub>00</sub>			1190.5 <sup>i</sup>	<b>1191.5</b>
<b>MAD</b>	P	1 <sub>10</sub> ←1 <sub>01</sub>	<b>1185.9</b>	<b>1190.4</b>	1190.2 <sup>i</sup>	<b>1189.6</b>
		0 <sub>00</sub> ←1 <sub>01</sub>	1164.0 <sup>g</sup>	<b>1170.8</b>	1166.6 <sup>i</sup>	<b>1169.1</b>
	R		13.1	3.2	1.1	0
			24.4	7.9	5.7	0

<sup>a</sup>Bold face: obtained in the present study. Italics: Reference data. In green: tentative or new assignments. <sup>b</sup>VCI(SDTQ) on a 3-mode PES at CCSD(T)-F12/VTZ-F12. <sup>c</sup>Harmonic Approximation at CCSD(T)-F12/VTZ-F12. <sup>d</sup>Ref 17. <sup>e</sup>Ref 28. <sup>f</sup>Ref 32. <sup>g</sup>Ref 33. <sup>h</sup>Ref 62. <sup>i</sup>Ref 63. <sup>j</sup>Ref 64. <sup>k</sup>Ref 65. <sup>l</sup>Ref 66.

spectrum, we suggest that HDO  $\nu_3$  should be at roughly 3707  $\text{cm}^{-1}$ . This is not observed in our experiments and not reported in the experiments in refs 32 and 28. The band either red- or blueshifts by 7  $\text{cm}^{-1}$ . In our experiment, it seems to be basically split by 14  $\text{cm}^{-1}$ . VCI-calculated (and gas-phase) rovibs cannot explain the bands at 3699.0 and 3713.8  $\text{cm}^{-1}$ . Further experiments may verify whether the HDO  $\nu_3$  fundamental vibration can be found at 3707  $\text{cm}^{-1}$ . The HDO  $\nu_1$  is assigned at 2722.9  $\text{cm}^{-1}$  in ref 28, which is in excellent agreement with our VCI calculations. Ceponkus et al.<sup>32</sup> claim it to be at 2727.5  $\text{cm}^{-1}$ . This band, however, is astonishingly close to a transition observed in ref 28 for HD<sup>18</sup>O species (2727.7  $\text{cm}^{-1}$ ). In our experiment, HD<sup>18</sup>O can be clearly ruled out. If naturally occurring <sup>18</sup>O was the origin,

then we should observe a 1000-fold more intense HD<sup>16</sup>O band, which is not the case. Also, rovibs can be excluded based on our VCI calculations and gas-phase reference. As shown in Figure 2, there are some bands in the 2729–2727  $\text{cm}^{-1}$  region and a weak band at 2718.9  $\text{cm}^{-1}$ , which is indirectly proportional to the sample concentration. The observed bands must have a different origin and do not represent fundamental vibs or rovibs of the water monomer. The origin of this remains unclear—it might be explained based on oligomers or effects not considered in our calculation, for example, a splitting caused by different kinds of matrix cages.

Besides the improved spectroscopic assignment, the VCI wave function allows for the computation of vibrationally averaged structural parameters,<sup>67,68</sup> here collectively abbreviated as  $r_{Av}$  and not to be confused with equilibrium structural parameters, abbreviated as  $r_E$ , from geometry optimization within the Born–Oppenheimer approximation. In Table 3,  $r_{Av}$

**Table 3. Calculated and Experimental Gas-phase Structural Parameters of Water<sup>a</sup>**

Mol.	Parameter	Calculated			Experimental	
		$r_E^b$	$r_{Av}^c$	$r_{Av}^d$	MW <sup>e</sup>	GEP <sup>f</sup>
<b>H<sub>2</sub>O</b>	r(OH) / Å	<b>0.9586</b>	<b>0.9736</b>	0.9757	0.9724	0.976 ± 0.003
	α(HOH) / °	<b>104.40</b>	<b>104.30</b>	104.43	104.50	107.3 ± 3
	A / $\text{cm}^{-1}$	<b>27.2810</b>	<b>27.7551</b>	27.8656	27.8825	
	B / $\text{cm}^{-1}$	<b>14.5763</b>	<b>14.4985</b>	14.5042	14.5153	
<b>HDO</b>	C / $\text{cm}^{-1}$	<b>9.5003</b>	<b>9.2681</b>	9.2964	9.2824	
	r(OH) / Å	<b>0.9586</b>	<b>0.9722</b>			
	r(OD) / Å	<b>0.9586</b>	<b>0.9704</b>			
	α(DOH) / °	<b>104.40</b>	<b>104.31</b>			
<b>D<sub>2</sub>O</b>	A / $\text{cm}^{-1}$	<b>23.0477</b>	<b>23.3152</b>		23.4143	
	B / $\text{cm}^{-1}$	<b>9.1158</b>	<b>9.0853</b>		9.1012	
	C / $\text{cm}^{-1}$	<b>6.5322</b>	<b>6.4008</b>		6.4084	
	r(OD) / Å	<b>0.9586</b>	<b>0.9695</b>	0.9708	0.9687	0.970 ± 0.003
<b>D<sub>2</sub>O</b>	α(DOD) / °	<b>104.40</b>	<b>104.29</b>	104.41	104.35	104.2 ± 3
	A / $\text{cm}^{-1}$	<b>15.1760</b>	<b>15.3472</b>	15.4139	15.4204	
	B / $\text{cm}^{-1}$	<b>7.2935</b>	<b>7.2637</b>	7.2730	7.2711	
	C / $\text{cm}^{-1}$	<b>4.9261</b>	<b>4.8382</b>	4.8463	4.8467	

<sup>a</sup>Bold face: obtained in the present study. Italics: Reference data. <sup>b</sup>Geometry optimization at CCSD(T)-F12/VTZ-F12. <sup>c</sup>Vibrational Ground State from VCI(SDTQ) on a 3-mode PES at CCSD(T)-F12/VTZ-F12. <sup>d</sup>Calculations by Czako et al. <sup>e</sup>Microwave experiments in Ref. 70. <sup>f</sup>Gas-phase electron diffraction experiments in Ref. 71.

and  $r_E$  from the present multimode PES-based VSCF/VCI calculation and from the extensive calculations by Czako et al.<sup>68</sup> on an adiabatic semiglobal PES<sup>69</sup> are listed together with structural parameters deduced from microwave (MW) spectroscopy<sup>70</sup> and gas-phase electron diffraction (GED) experiments.<sup>71</sup> The experimental structural parameters from MW, for example, the rotational constants A, B, and C for all three isotopomers, are in a much better agreement with the computed  $r_{Av}$  than with the computed  $r_E$ , for both the calculations by Czako et al.<sup>68</sup> and the present VCI calculations. The  $r_E$  bond length and angle are the same for all three isotopomers, as the Born–Oppenheimer PES is mass-independent. In experiments, however, bond lengths and angles are not observed as mass-independent. Both in MW and in GED experiments, a difference of roughly 0.06 Å between  $r(\text{OH})$  and  $r(\text{OD})$  is observed. This experimentally observed mass dependency is also reproduced in the calculated  $r_{Av}$  bond lengths. Although a comparison of ab initio computed with spectroscopically deduced structural parameters is involved—we refer to Császár et al.<sup>72</sup> for a discussion on the pitfalls of such comparison—the good agreement substantiates the

physical validity of the present VCI approach and it is clear evidence that anharmonicity significantly impacts the observed molecular structure.

#### 4. CONCLUSIONS

Our results demonstrate that deviations of computed vibrational spectra to experimental spectra are minimized when anharmonicity and mode coupling are incorporated with a multimode PES representation and the time-independent nuclear Schrödinger equation is solved with the variational VSCF/VCI approach. This approach allows for a prediction of pure vibrational transitions with an error of just  $1\text{ cm}^{-1}$  on average and is also suitable for describing the challenging situation of a molecule rotating in the matrix cage when the rotation is not too hindered as in the case of water. Only this accuracy allows us to confidently assign every single observed band, identify inconsistencies in the state-of-the-art assignment, and to reassign some bands in the Ne MI-IR spectrum of the HDO species. From our MI-IR experiments, we gain profound understanding of matrix-shifts where Ne shifts are rather small with a difference to the gas phase of only  $1.5\text{ cm}^{-1}$  on average. With Ne MI-IR being close to the gas-phase situation and the capability of the VSCF/VCI approach to accurately predict gas-phase transitions, we encounter a powerful combination of experiment and theory. Even for water that has been studied for more than 60 years by MI-IR spectroscopy and theoretical calculations, our combined approach has allowed us to improve our understanding of the rotational–vibrational transitions. The theoretical framework and the way to include anharmonicity as employed here will allow for sound assignments of many small molecules studied by MI-IR spectroscopy. The benefit will become even more evident for molecules where exact solutions are not yet available in the literature.

#### ■ ASSOCIATED CONTENT

##### Supporting Information

The Supporting Information is available free of charge on the ACS Publications website at DOI: 10.1021/acs.jpca.9b07221.

Assignment of water monomers and dimers in argon and neon MI-IR spectra and directly observed transitions of water dimers (PDF)

#### ■ AUTHOR INFORMATION

##### Corresponding Authors

\*E-mail: hinrich.grothe@tuwien.ac.at (H.G.).

\*E-mail: klaus.liedl@uibk.ac.at (K.R.L.).

\*E-mail: thomas.loerting@uibk.ac.at (T.L.).

##### ORCID

Dennis F. Dinu: 0000-0001-8239-7854

Maren Podewitz: 0000-0001-7256-1219

Hinrich Grothe: 0000-0002-2715-1429

Klaus R. Liedl: 0000-0002-0985-2299

Thomas Loerting: 0000-0001-6694-3843

##### Notes

The authors declare no competing financial interest.

#### ■ ACKNOWLEDGMENTS

We gratefully acknowledge support by the Austrian Science Fund FWF (project I1392 and project P30565) and the Austria Research Promotion Agency FFG (bridge project

EARLYSNOW, 850689). M.P. would like to thank the FWF for a Lise Meitner Postdoctoral Fellowship (M-2005).

#### ■ REFERENCES

- (1) Rosenkranz, P. W. Water Vapor Microwave Continuum Absorption: A Comparison of Measurements and Models. *Radio Sci.* **1998**, *33*, 919–928.
- (2) Nedoluha, G. E.; Kiefer, M.; Lossow, S.; Gomez, R. M.; Kämpfer, N.; Lainer, M.; Forkman, P.; Christensen, O. M.; Oh, J. J.; Hartogh, P.; Anderson, J.; Bramstedt, K.; Dinelli, B. M.; Garcia-Comas, M.; Hervig, M.; Murtagh, D.; Raspollini, P.; Read, W. G.; Rosenlof, K.; Stiller, G. P.; Walker, K. A. The SPARC Water Vapor Assessment II: Intercomparison of Satellite and Ground-Based Microwave Measurements. *Atmos. Chem. Phys.* **2017**, *17*, 14543–14558.
- (3) Messer, J. K.; De Lucia, F. C.; Helminger, P. The Pure Rotational Spectrum of Water Vapor—A Millimeter, Submillimeter, and Far Infrared Analysis. *Int. J. Infrared Millimeter Waves* **1983**, *4*, 505–539.
- (4) Bernath, P. F. The Spectroscopy of Water Vapour: Experiment, Theory and Applications. *Phys. Chem. Chem. Phys.* **2002**, *4*, 1501–1509.
- (5) Tennyson, J.; Bernath, P. F.; Brown, L. R.; Campargue, A.; Császár, A. G.; Daumont, L.; Gamache, R. R.; Hodges, J. T.; Naumenko, O. V.; Polyansky, O. L.; Rothman, L. S.; Vandaele, A. C.; Zobov, N. F. A Database of Water Transitions from Experiment and Theory (IUPAC Technical Report). *Pure Appl. Chem.* **2014**, *86*, 71–83.
- (6) Tennyson, J.; Bernath, P. F.; Brown, L. R.; Campargue, A.; Carleer, M. R.; Császár, A. G.; Gamache, R. R.; Hodges, J. T.; Jenouvrier, A.; Naumenko, O. V.; et al. IUPAC Critical Evaluation of the Rotational–Vibrational Spectra of Water Vapor. Part I—Energy Levels and Transition Wavenumbers for  $\text{H}_2^{17}\text{O}$  and  $\text{H}_2^{18}\text{O}$ . *J. Quant. Spectrosc. Radiat. Transfer* **2009**, *110*, 573–596.
- (7) Tennyson, J.; Bernath, P. F.; Brown, L. R.; Campargue, A.; Császár, A. G.; Daumont, L.; Gamache, R. R.; Hodges, J. T.; Naumenko, O. V.; Polyansky, O. L.; et al. IUPAC Critical Evaluation of the Rotational–Vibrational Spectra of Water Vapor. Part II: Energy levels and transition wavenumbers for  $\text{HD}^{16}\text{O}$ ,  $\text{HD}^{17}\text{O}$ ,  $\text{HD}^{18}\text{O}$ . *J. Quant. Spectrosc. Radiat. Transfer* **2010**, *111*, 2160–2184.
- (8) Tennyson, J.; Bernath, P. F.; Brown, L. R.; Campargue, A.; Császár, A. G.; Daumont, L.; Gamache, R. R.; Hodges, J. T.; Naumenko, O. V.; Polyansky, O. L.; et al. IUPAC Critical Evaluation of the Rotational–Vibrational Spectra of Water Vapor, Part III: Energy Levels and Transition Wavenumbers for  $\text{H}_2^{16}\text{O}$ . *J. Quant. Spectrosc. Radiat. Transfer* **2013**, *117*, 29–58.
- (9) Tennyson, J.; Bernath, P. F.; Brown, L. R.; Campargue, A.; Császár, A. G.; Daumont, L.; Gamache, R. R.; Hodges, J. T.; Naumenko, O. V.; Polyansky, O. L.; et al. IUPAC Critical Evaluation of the Rotational–Vibrational Spectra of Water Vapor. Part IV. Energy Levels and Transition Wavenumbers for  $\text{D}_2^{16}\text{O}$ ,  $\text{D}_2^{17}\text{O}$ , and  $\text{D}_2^{18}\text{O}$ . *J. Quant. Spectrosc. Radiat. Transfer* **2014**, *142*, 93–108.
- (10) Van Thiel, M.; Becker, E. D.; Pimentel, G. C. Infrared Studies of Hydrogen Bonding of Water by the Matrix Isolation Technique. *J. Chem. Phys.* **1957**, *27*, 486–490.
- (11) Catalano, E.; Milligan, D. E. Infrared Spectra of  $\text{H}_2\text{O}$ ,  $\text{D}_2\text{O}$ , and HDO in Solid Argon, Krypton, and Xenon. *J. Chem. Phys.* **1959**, *30*, 45–47.
- (12) Glasel, J. A. Near-Infrared Absorption Spectra of Ortho- and Para- $\text{H}_2\text{O}$  in Solid Xenon and Argon. *J. Chem. Phys.* **1960**, *33*, 252–255.
- (13) Redington, R. L.; Milligan, D. E. Infrared Spectroscopic Evidence for the Rotation of the Water Molecule in Solid Argon. *J. Chem. Phys.* **1962**, *37*, 2162.
- (14) Redington, R. L.; Milligan, D. E. Molecular Rotation and Ortho—Para Nuclear Spin Conversion of Water Suspended in Solid Ar, Kr, and Xe. *J. Chem. Phys.* **1963**, *39*, 1276–1284.
- (15) Hopkins, H. P., Jr.; Curl, R. F., Jr.; Pitzer, K. S. Infrared Matrix-Isolation Studies of Nuclear-Spin-Species Conversion. *J. Chem. Phys.* **1968**, *48*, 2959–2965.

- (16) Tursi, A. J.; Nixon, E. R. Matrix-Isolation Study of the Water Dimer in Solid Nitrogen. *J. Chem. Phys.* **1970**, *52*, 1521–1528.
- (17) Ayers, G. P.; Pullin, A. D. E. Reassignment of the Vibrational Spectra of Matrix Isolated H<sub>2</sub>O and HDO. *Chem. Phys. Lett.* **1974**, *29*, 609–615.
- (18) Ayers, G. P.; Pullin, A. D. E. The I.R. Spectra of Matrix Isolated Water Species-I. Assignment of Bands to (H<sub>2</sub>O)<sub>2</sub>, (D<sub>2</sub>O)<sub>2</sub> and HDO Dimer Species in Argon Matrices. *Spectrochim. Acta, Part A* **1976**, *32*, 1629–1639.
- (19) Ayers, G. P.; Pullin, A. D. E. The I.R. Spectra of Matrix Isolated Water Species-II. The Characterisation of Non-Rotating Monomer Water Species in an Argon Matrix by Xenon Doping: The Matrix Isolated Spectra of H<sub>2</sub>O·HCl and (CH<sub>3</sub>)<sub>2</sub>O·H<sub>2</sub>O as Model Compounds for Water Dimer Spectra. *Spectrochim. Acta, Part A* **1976**, *32*, 1641–1650.
- (20) Ayers, G. P.; Pullin, A. D. E. The I.R. Spectra of Matrix Isolated Water Species-III. Infrared Spectra and Assignments of <sup>18</sup>O Containing Monomer and Dimer Water Species in Argon Matrices. *Spectrochim. Acta, Part A* **1976**, *32*, 1689–1693.
- (21) Ayers, G. P.; Pullin, A. D. E. The I.R. Spectra of Matrix Isolated Water Species-IV. The Configuration of the Water Dimer in Argon Matrices. *Spectrochim. Acta, Part A* **1976**, *32*, 1695–1704.
- (22) Pfeilsticker, K.; Lotter, A.; Peters, C.; Bösch, H. Atmospheric Detection of Water Dimers via Near-Infrared Absorption. *Science* **2003**, *300*, 2078–2080.
- (23) Mukhopadhyay, A.; Cole, W. T. S.; Saykally, R. J. The Water Dimer I: Experimental Characterization. *Chem. Phys. Lett.* **2015**, *633*, 13–26.
- (24) Mukhopadhyay, A.; Xantheas, S. S.; Saykally, R. J. The Water Dimer II: Theoretical Investigations. *Chem. Phys. Lett.* **2018**, *700*, 163–175.
- (25) Bentwood, R. M.; Barnes, A. J.; Orville-Thomas, W. J. Studies of Intermolecular Interactions by Matrix Isolation Vibrational Spectroscopy: Self-Association of Water. *J. Mol. Spectrosc.* **1980**, *84*, 391–404.
- (26) Nelander, B. The Intramolecular Fundamentals of the Water Dimer. *J. Chem. Phys.* **1988**, *88*, 5254–5256.
- (27) Perchard, J. P. Anharmonicity and Hydrogen Bonding. III. Analysis of the Near Infrared Spectrum of Water Trapped in Argon Matrix. *Chem. Phys.* **2001**, *273*, 217–233.
- (28) Forney, D.; Jacox, M. E.; Thompson, W. E. The Mid- and Near-Infrared Spectra of Water and Water Dimer Isolated in Solid Neon. *J. Mol. Spectrosc.* **1993**, *157*, 479–493.
- (29) Ceponkus, J.; Nelander, B. Water Dimer in Solid Neon. Far-Infrared Spectrum. *J. Phys. Chem. A* **2004**, *108*, 6499–6502.
- (30) Bouteiller, Y.; Tremblay, B.; Perchard, J. P. The Vibrational Spectrum of the Water Dimer: Comparison between Anharmonic Ab Initio Calculations and Neon Matrix Infrared Data between 14,000 and 90 cm<sup>-1</sup>. *Chem. Phys.* **2011**, *386*, 29–40.
- (31) Tremblay, B.; Madebène, B.; Alikhani, M. E.; Perchard, J. P. The Vibrational Spectrum of the Water Trimer: Comparison between Anharmonic Ab Initio Calculations and Neon Matrix Infrared Data between 11,000 and 90 cm<sup>-1</sup>. *Chem. Phys.* **2010**, *378*, 27–36.
- (32) Ceponkus, J.; Uvdal, P.; Nelander, B. The Coupling between Translation and Rotation for Monomeric Water in Noble Gas Matrices. *J. Chem. Phys.* **2013**, *138*, 244305.
- (33) Engdahl, A.; Nelander, B. Water in Krypton Matrices. *J. Mol. Struct.* **1989**, *193*, 101–109.
- (34) Givan, A.; Grothe, H.; Loewenschuss, A.; Nielsen, C. J. Infrared Spectra and Ab Initio Calculations of Matrix Isolated Dimethyl Sulfone and Its Water Complex. *Phys. Chem. Chem. Phys.* **2002**, *4*, 255–263.
- (35) Császár, A. G.; Mills, I. M. Vibrational Energy Levels of Water. *Spectrochim. Acta, Part A* **1997**, *53*, 1101–1122.
- (36) Polyansky, O. L.; Császár, A. G.; Shirin, S. V.; Zobov, N. F.; Barletta, P.; Tennyson, J.; Schwenke, D. W.; Knowles, P. J. High-Accuracy Ab Initio Rotation-Vibration Transitions for Water. *Science* **2003**, *299*, 539–542.
- (37) Barber, R. J.; Tennyson, J.; Harris, G. J.; Tolchenov, R. N. A High-Accuracy Computed Water Line List. *Mon. Not. R. Astron. Soc.* **2006**, *368*, 1087–1094.
- (38) Polyansky, O. L.; Zobov, N. F.; Mizus, I. I.; Lodi, L.; Yurchenko, S. N.; Tennyson, J.; Császár, A. G.; Boyarkin, O. V. Global Spectroscopy of the Water Monomer. *Philos. Trans. R. Soc., A* **2012**, *370*, 2728–2748.
- (39) Panchenko, Y. N. Vibrational Spectra and Scaled Quantum-Mechanical Molecular Force Fields. *J. Mol. Struct.* **2001**, *567*–568, 217–230.
- (40) Pulay, P.; Fogarasi, G.; Pongor, G.; Boggs, J. E.; Vargha, A. Combination of Theoretical Ab Initio and Experimental Information to Obtain Reliable Harmonic Force Constants. Scaled Quantum Mechanical (QM) Force Fields for Glyoxal, Acrolein, Butadiene, Formaldehyde, and Ethylene. *J. Am. Chem. Soc.* **1983**, *105*, 7037–7047.
- (41) Carney, G. D.; Sprandel, L. L.; Kern, C. W. Variational Approaches to Vibration-Rotation Spectroscopy for Polyatomic Molecules. *Adv. Chem. Phys.* **1978**, *37*, 305.
- (42) Bowman, J. M. The Self-Consistent-Field Approach to Polyatomic Vibrations. *Acc. Chem. Res.* **1986**, *19*, 202–208.
- (43) Ratner, M. A.; Gerber, R. B. Excited Vibrational States of Polyatomic Molecules: The Semiclassical Self-Consistent Field Approach. *J. Phys. Chem.* **1986**, *90*, 20–30.
- (44) Jung, J. O.; Gerber, R. B. Vibrational Wave Functions and Spectroscopy of (H<sub>2</sub>O)<sub>n</sub>, n=2,3,4,5: Vibrational Self-Consistent Field with Correlation Corrections. *J. Chem. Phys.* **1996**, *105*, 10332–10348.
- (45) Christiansen, O. Vibrational Structure Theory: New Vibrational Wave Function Methods for Calculation of Anharmonic Vibrational Energies and Vibrational Contributions to Molecular Properties. *Phys. Chem. Chem. Phys.* **2007**, *9*, 2942.
- (46) Christiansen, O. Selected New Developments in Vibrational Structure Theory: Potential Construction and Vibrational Wave Function Calculations. *Phys. Chem. Chem. Phys.* **2012**, *14*, 6672.
- (47) Rauhut, G. Efficient Calculation of Potential Energy Surfaces for the Generation of Vibrational Wave Functions. *J. Chem. Phys.* **2004**, *121*, 9313–9322.
- (48) Rauhut, G. Configuration Selection as a Route towards Efficient Vibrational Configuration Interaction Calculations. *J. Chem. Phys.* **2007**, *127*, 184109.
- (49) Rauhut, G.; Hartke, B. Modeling of High-Order Many-Mode Terms in the Expansion of Multidimensional Potential Energy Surfaces: Application to Vibrational Spectra. *J. Chem. Phys.* **2009**, *131*, 014108.
- (50) Oschetzki, D.; Neff, M.; Meier, P.; Pfeiffer, F.; Rauhut, G. Selected Aspects Concerning the Efficient Calculation of Vibrational Spectra beyond the Harmonic Approximation. *Croat. Chem. Acta* **2012**, *85*, 379–390.
- (51) Gálvez, O.; Zoerner, A.; Loewenschuss, A.; Grothe, H. A Combined Matrix Isolation and Ab Initio Study of Bromine Oxides. *J. Phys. Chem. A* **2006**, *110*, 6472–6481.
- (52) Bernard, J.; Seidl, M.; Kohl, I.; Liedl, K. R.; Mayer, E.; Gálvez, Ó.; Grothe, H.; Loerting, T. Spectroscopic Observation of Matrix-Isolated Carbonic Acid Trapped from the Gas Phase. *Angew. Chem., Int. Ed.* **2011**, *50*, 1939–1943.
- (53) Gifford, W. E.; Longworth, R. C. *Surface Heat Pumping BT - Advances in Cryogenic Engineering*; Timmerhaus, K. D., Ed.; Springer US: Boston, MA, 1966; pp 171–179.
- (54) Werner, H.-J.; Knowles, P. J.; Knizia, G.; Manby, F. R.; Schütz, M. Molpro: A General Purpose Quantum Chemistry Program Package. *Wiley Interdiscip. Rev.: Comput. Mol. Sci.* **2012**, *2*, 242–253.
- (55) Werner, H.-J.; Knowles, P. J.; Knizia, G.; Manby, F. R.; Schütz, M.; Celani, P.; Györfy, W.; Kats, D.; Korona, T.; Lindh, R.; et al. MOLPRO, Version 2015.1, a Package of Ab Initio Programs. University of Cardiff Chemistry Consultants (UC3): Cardiff, Wales, UK, 2015.
- (56) Adler, T. B.; Knizia, G.; Werner, H.-J. A Simple and Efficient CCSD(T)-F12 Approximation. *J. Chem. Phys.* **2007**, *127*, 221106.

(57) Knizia, G.; Adler, T. B.; Werner, H.-J. Simplified CCSD(T)-F12 Methods: Theory and Benchmarks. *J. Chem. Phys.* **2009**, *130*, No. 054104.

(58) Peterson, K. A.; Adler, T. B.; Werner, H.-J. Systematically Convergent Basis Sets for Explicitly Correlated Wavefunctions: The Atoms H, He, B-Ne, and Al-Ar. *J. Chem. Phys.* **2008**, *128*, No. 084102.

(59) Yousaf, K. E.; Peterson, K. A. Optimized Auxiliary Basis Sets for Explicitly Correlated Methods. *J. Chem. Phys.* **2008**, *129*, 184108.

(60) Rauhut, G.; Knizia, G.; Werner, H.-J. Accurate Calculation of Vibrational Frequencies Using Explicitly Correlated Coupled-Cluster Theory. *J. Chem. Phys.* **2009**, *130*, No. 054105.

(61) Carter, S.; Bowman, J. M. The Adiabatic Rotation Approximation for Rovibrational Energies of Many-Mode Systems: Description and Tests of the Method. *J. Chem. Phys.* **1998**, *108*, 4397–4404.

(62) Toth, R. A. Analysis of Line Positions and Strengths of H<sub>2</sub><sup>16</sup>O Ground and Hot Bands Connecting to Interacting Upper States: (020), (100), and (001). *J. Mol. Spectrosc.* **1999**, *194*, 28–42.

(63) Toth, R. A. Water Vapor Measurements between 590 and 2582 Cm<sup>-1</sup>: Line Positions and Strengths. *J. Mol. Spectrosc.* **1998**, *190*, 379–396.

(64) Toth, R. A.; Gupta, V. D.; Brault, J. W. Line Positions and Strengths of HDO in the 2400–3300-cm<sup>-1</sup> Region. *Appl. Opt.* **1982**, *21*, 3337–3347.

(65) Toth, R. A. HDO and D<sub>2</sub>O Low Pressure, Long Path Spectra in the 600-3100 cm<sup>-1</sup> Region: I. HDO Line Positions and Strengths. *J. Mol. Spectrosc.* **1999**, *195*, 73–97.

(66) Toth, R. A. HDO and D<sub>2</sub>O Low Pressure, Long Path Spectra in the 600-3100 cm<sup>-1</sup> Region: II. D<sub>2</sub>O Line Positions and Strengths. *J. Mol. Spectrosc.* **1999**, *195*, 98–122.

(67) Rauhut, G. Anharmonic Franck–Condon Factors for the  $\tilde{X}^2B_1 \leftarrow \tilde{X}^1A_1$  Photoionization of Ketene. *J. Phys. Chem. A* **2015**, *119*, 10264–10271.

(68) Czakó, G.; Mátyus, E.; Császár, A. G. Bridging Theory with Experiment: A Benchmark Study of Thermally Averaged Structural and Effective Spectroscopic Parameters of the Water Molecule. *J. Phys. Chem. A* **2009**, *113*, 11665–11678.

(69) Barletta, P.; Shirin, S. V.; Zobov, N. F.; Polyansky, O. L.; Tennyson, J.; Valeev, E. F.; Császár, A. G. CVRQD Ab Initio Ground-State Adiabatic Potential Energy Surfaces for the Water Molecule. *J. Chem. Phys.* **2006**, *125*, 204307.

(70) Cook, R. L.; De Lucia, F. C.; Helminger, P. Molecular Force Field and Structure of Water: Recent Microwave Results. *J. Mol. Spectrosc.* **1974**, *53*, 62–76.

(71) Shibata, S.; Bartell, L. S. Electron-Diffraction Study of Water and Heavy Water. *J. Chem. Phys.* **1965**, *42*, 1147–1151.

(72) Császár, A. G.; Czakó, G.; Furtenbacher, T.; Tennyson, J.; Szalay, V.; Shirin, S. V.; Zobov, N. F.; Polyansky, O. L. On Equilibrium Structures of the Water Molecule. *J. Chem. Phys.* **2005**, *122*, 214305.